BNL-104790-2014-TECH

AGS/AD/Tech Note No. 374;BNL-104790-2014-IR

THREE DIMENSIONAL FIELD ANALYSIS FOR THE AGS COMBINED FUNCTION MAGNETS

W. Meng

April 1993

Collider Accelerator Department

Brookhaven National Laboratory

U.S. Department of Energy

USDOE Office of Science (SC)

DISCLAIMER

Accelerator Division
Alternating Gradient Synchrotron Department
BROOKHAVEN NATIONAL LABORATORY
Upton, New York 11973

Accelerator Division
Technical Note

AGS/AD/Tech. Note No. 374

THREE-DIMENSIONAL FIELD ANALYSIS FOR THE AGS COMBINED FUNCTION MAGNETS

W. Meng and M. Tanaka

April 12, 1993

Three Dimensional Field Analysis for the AGS Combined Function Magnets

W. Meng and M. Tanaka

Introduction

The design of the AGS new fast extraction beam (NewFEB) system for the g-2 experiment and RHIC injection[1] requires detailed magnetic field knowledge about the AGS main magnets, so that one may predict the trajectories of 29 GeV/c protons in the fringe field region during the extraction (Fig.1). 2d and 3d magnetic field computations have been done by using POISSON code and TOSCA programs. Partial results are described in this note. The comparisons between calculated field values and measured field maps show that if one properly handles the TOSCA program, high accuracy can be achieved. Further studies will show that particle tracking by using the post process of the TOSCA program is feasible[2].

POISSON Calculations

The pole surface of the AGS magnets was well designed many years ago, based on a constant magnetic scalar potential surface. The material of the magnets is the Electrical Grade M-36 Steel which contains 1.80% silicon and 0.03% carbon. The packing factor of the laminations is about 0.98[3]. To simulate the magnets in 2d calculation, 51 points are used to define the curve of the pole surface (Fig.2), according to the final design[4]. The B-H data of the POISSON input is based on a measured magnetization curve. It was interporated in order to ensure the smoothness of its first derivatives and the continuity of its second derivatives.

Figure 3 and 4 are the plots of the computed vertical component of the magnetic induction B_y and its gradient on the median plane versus the transverse coordinate x, for the "open" and "closed" types AGS magnets respectively.

Table 1 is the list of the data; table 2 is the harmonic content. The origin of the coordinates is located at the central orbit, so that it is ± 2 inches deviated from the geometrical center of the pole, depending on the "closed" or the "open" type of magnets. The positive x direction is pointing the ring center.

In principle, 2d computations should be comparable with the measurements near the middle of the magnet. Figure 5 shows the absolute comparison between the POISSON results and the measured data, in the case of feeding 41000 ampere per coil. The measurement[5] was performed at the location of 27 inch into the magnet from the end face. One can hardly recognize that there are two curves in the figure; the measured curve is superimposed on the computed curve, from $x = -20cm$ to $x = 18cm$. The disagreement is less than 2 part per thousand.

TOSCA Calculations

The advent of relatively inexpensive and powerful computers has inspired the development of the large scale three dimensional codes. TOSCA is one of the most well known commercial codes which is widely used in the industry and accelerator field.

Based on the reference [4], a finite element model of one-quarter of the "open" type AGS magnet was constructed. Figure 6 only shows the steel part. The origin of the coordinate system of the TOSCA calculations is in the middle of the magnet and also at the beam center. The positive x direction is pointing the ring center.

Figure 7 shows the landscape plot of the vertical components of B-field on the median plane, around the edge of the magnet. The base area 1-2-3-4 stands for the part of the median plane. The cartesian and polar coordinates of these four corners are listed on the right side of the figure. The vertical height of the surface stands for the magnitude of the component B_y at particular position on the median plane. On the base area, there is a family of curves which represents the equal-height contours (or constant B_y lines).

Figure 8(a) is the same subject but from different view point. Using a set of $x = const.$

planes to cut this surface, one gets a set of curves which represents the variations of B_y along the axial direction z, at different transverse location x; that is shown in Figure 8(b).

Followings are part of the comparisons between the TOSCA results and the measured data.

(a) Compare with the low field measurements:

Measured data file AGBU01.MPA[5] is the field map with the applied current 2880 ampere per coil. The center field is about 815 gauss, corresponding to 2 GeV/c protons. Figure 9 shows the comparison between the measured data and the calculation, on the median plane, near the center of the magnet. The difference is about 0.6%. Figure 10 shows the comparison along the central beam line; the difference is about 0.7%. Figure 11 shows the comparison in the fringe field region (6 inch away from the center); the difference is about 0.3%.

(b) Compare with the high field measurements:

Measured data file B5150A.MPA[5] is the field map of a open type AGS magnet; the applied current is 41000 ampere per coil (5150 ampere per pair), corresponding to 29 GeV/c protons.

Measured data file A5150A.MPA[5] is again the field map of a open type AGS magnet, except it measured only in the fringe field region along the open side of the magnet.

Figure 12 shows the comparison between the above two measured field maps and the TOSCA calculated results. The measured data B5150A.MPA covers from $x = 0cm$ to $x = 18cm$. The difference between this measured data and the calculation is about 0.5%.

The measured data A5150A.MPA covers from $x = -40cm$ to $0cm$, It is noticed that near the point $x = -9.14cm$, the second order derivative shows some discontinuity. Accordingly one may estimate that the measurements error could be about 1.1 %. These prossibly arose from relocating the equipment and remaining magnetization in the steel core during the measurements.

Conclusions

Authors like to comment the TOSCA program and computations on the following points.

(a)Time Consumption. The time cost for constructing the finite element model depends on the problem size, complexity and the experience of the user. The computer CPU time has reduced tremendously since softwares are available on the UNIX machine (IBM RISC System). General speaking, to obtain a field map with a reasonable accuracy, it takes less man power by using TOSCA program than by carrying out a measurement. Nevertheless measurements are always indispensable, since it is the most important way to examine the computed results, as long as the magnet is existing and accessible.

(b)The Accuracy of the TOSCA program. The local error at a field point is determined by (1) the size of the elements surrounding the point; (2) the types of these elements (linear or quadratic); (3) the method required to calculate the field value from the potential array (differentiation of shape function, interpolation of nodal averaged values, or integration of magnetization and currents); (4) the far boundary conditions and the potential types. From first glance, one could say that the accuracy is strongly linked to the size of the elements which is limited by the capacity of the program, but this is not the only factor. By making correct choices from factors (2), (3) and (4), reasonablely high accuracy is achievable. According to the results presented in this note, the error of the TOSCA computation is within the error of the measurements.

Acknowledgment

Authors appreciate the AGS initiator G. Danby for his instructive guidance and discussion.

Authors appreciate R. Thern who reserves useful measured data files about the AGS magnets.

References

[1] M. Tanaka and Y.Y. Lee, BNL-45344.

[2] W. Meng and M. Tanaka, to be published.

[3] Alternating Gradient Synchrotron Project Construction Completion Report, December 1966.

[4] Engineering Drawing D03-M-666-5, D03-M-667-5.

[5] R. Thern, private communication.

Table I. Vertical Field Components for AGS Main Magnets

x [cm]*	Open Magnets By (x,y) [gauss] y=0.0 [cm]	y=1.0 [cm]	y=2.0 [cm]	Closed Magnets By(x,y) [gauss] y=0.0 [cm]	y=1.0 [cm]	y=2.0 [cm]
35.00	244.632	239.466	223.925	785.695	776.259	747.850
34.00	301.328	295.228	276.931	932.274	922.617	893.768
33.00	370.183	363.271	342.328	1098.166	1088.256	1058.721
32.00	452.818	445.266	422.320	1283.912	1273.492	1242.769
31.00	550.472	542.569	518.569	1490.450	1479.323	1446.348
30.00	663.821	655.869	631.774	1719.414	1707.091	1670.726
29.00	793.047	785.235	761.674	1973.055	1959.154	1917.877
28.00	937.913	930.268	907.438	2254.800	2238.668	2190.938
27.00	1098.095	1090.578	1068.228	2569.028	2549.987	2493.833
26.00	1273.259	1265.804	1243.546	2921.500	2898.770	2831.697
25.00	1463.405	1455.820	1433.186	3319.617	3292.221	3211.361
24.00	1668.807	1660.932	1637.478	3772.779	3739.449	3641.404
23.00	1889.943	1881.671	1856.988	4292.803	4252.244	4132.332
22.00	2127.637	2118.876	2092.660	4894.441	4844.593	4697.530
21.00	2382.887	2373.563	2345.599	5596.369	5535.019	5353.894
20.00	2656.780	2646.880	2617.183	6421.036	6345.638	6122.979
19.00	2950.410	2939.995	2908.684	7396.535	7305.250	7032.310
18.00	3264.814	3253.994	3221.423	8552.403	8447.557	8122.647
17.00	3600.770	3589.685	3556.330	9915.666	9807.535	9451.888
16.00	3958.753	3947.593	3914.042	11481.799	11407.714	11102.826
15.00	4338.768	4327.813	4294.694	13175.547	13210.624	13199.825
14.00	4740.682	4730.146	4698.153	14768.125	15007.391	15820.633
13.00	5163.292	5153.606	5124.052	15909.600	16280.121	17715.729
12.00	5605.211	5596.860	5571.313	16384.783	16657.109	17498.480
11.00	6063.407	6056.943	6037.325	16328.815	16453.025	16730.533
10.00	6534.635	6530.239	6517.411	16007.716	16048.703	16120.461
9.00	7014.367	7012.097	7005.739	15587.454	15599.275	15617.825
8.00	7498.847	7498.239	7496.838	15136.125	15140.246	15147.791
7.00	7985.068	7985.333	7986.693	14674.849	14677.166	14683.707
6.00	8470.950	8471.586	8473.793	14207.441	14209.338	14214.270
5.00	8955.844	8956.468	8958.577	13737.682	13738.977	13742.769
4.00	9439.421	9440.046	9441.787	13265.366	13266.585	13269.677
3.00	9921.684	9922.247	9923.905	12791.472	12792.308	12794.375
2.00	10402.404	10402.954	10404.606	12316.388	12316.983	12318.443
1.00	10882.283	10882.765	10883.952	11840.263	11840.775	11843.048
0.00	11361.619	11362.159	11363.499	11362.364	11362.851	11364.327
-1.00	11840.651	11841.078	11843.138	10882.892	10883.339	10884.604
-2.00	12318.153	12318.751	12320.903	10402.511	10402.805	10403.710
-3.00	12794.440	12794.876	12796.305	9921.133	9921.553	9922.514
-4.00	13268.961	13269.594	13271.661	9439.495	9439.985	9441.522
-5.00	13740.710	13742.242	13746.963	8956.825	8957.482	8959.596
-6.00	14209.702	14210.975	14215.276	8473.038	8473.546	8475.479
-7.00	14675.072	14677.305	14682.614	7988.221	7988.239	7988.880
-8.00	15136.611	15141.147	15149.455	7503.607	7502.634	7500.334
-9.00	15587.577	15600.431	15620.565	7021.134	7018.613	7011.376
-10.00	16007.016	16048.773	16123.991	6544.021	6539.447	6525.798

* In this table, the positive x means away from the center of the AGS ring.

TABLE 2. HARMONIC CONTENT

NORMALIZATION RADIUS = 3.35000

(BX - I BY) = I * SUM N*(AN + I BN)/R * (Z/R)**(N-1)

Closed Type

N	N(AN)/R	N(BN)/R	ABS(N(CN)/R)
1	-1.1362E+04	0.0000E+00	1.1362E+04
2	1.6035E+03	0.0000E+00	1.6035E+03
3	6.1214E+00	0.0000E+00	6.1214E+00
4	-1.3904E+00	0.0000E+00	1.3904E+00
5	6.0634E-01	0.0000E+00	6.0634E-01
6	1.7675E-01	0.0000E+00	1.7675E-01
7	-5.5676E-01	0.0000E+00	5.5676E-01
8	-4.6347E-01	0.0000E+00	4.6347E-01
9	9.2682E-01	0.0000E+00	9.2682E-01
10	-5.4988E-01	0.0000E+00	5.4988E-01

Open Type

N	N(AN)/R	N(BN)/R	ABS(N(CN)/R)
1	-1.1362E+04	0.0000E+00	1.1362E+04
2	-1.6044E+03	0.0000E+00	1.6044E+03
3	5.4895E+00	0.0000E+00	5.4895E+00
4	1.2844E+00	0.0000E+00	1.2844E+00
5	8.3096E-01	0.0000E+00	8.3096E-01
6	-8.6606E-01	0.0000E+00	8.6606E-01
7	-4.9661E-01	0.0000E+00	4.9661E-01
8	-1.8460E-01	0.0000E+00	1.8460E-01
9	4.6949E-01	0.0000E+00	4.6949E-01
10	2.3566E-01	0.0000E+00	2.3566E-01

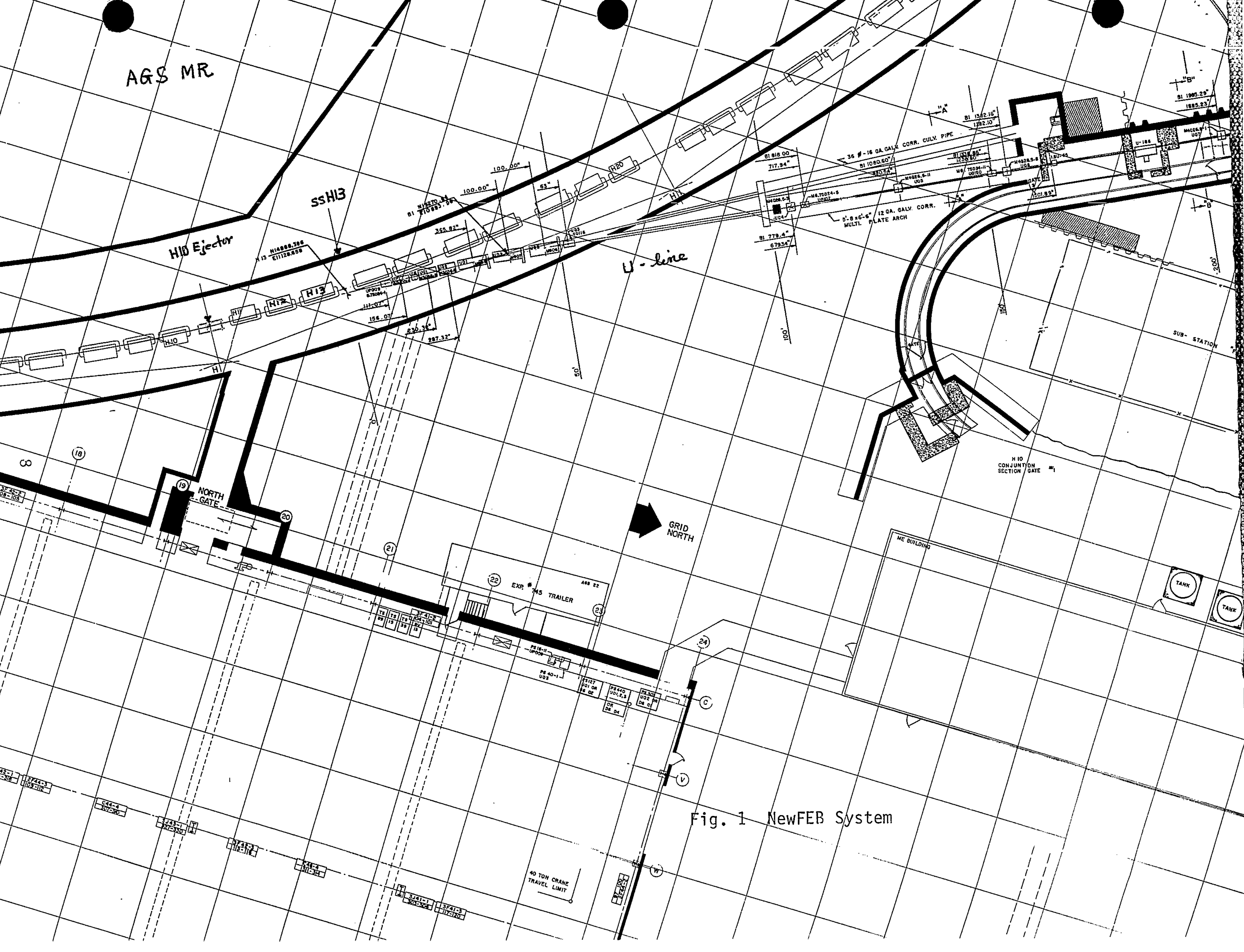

Fig. 1 NewFEB System

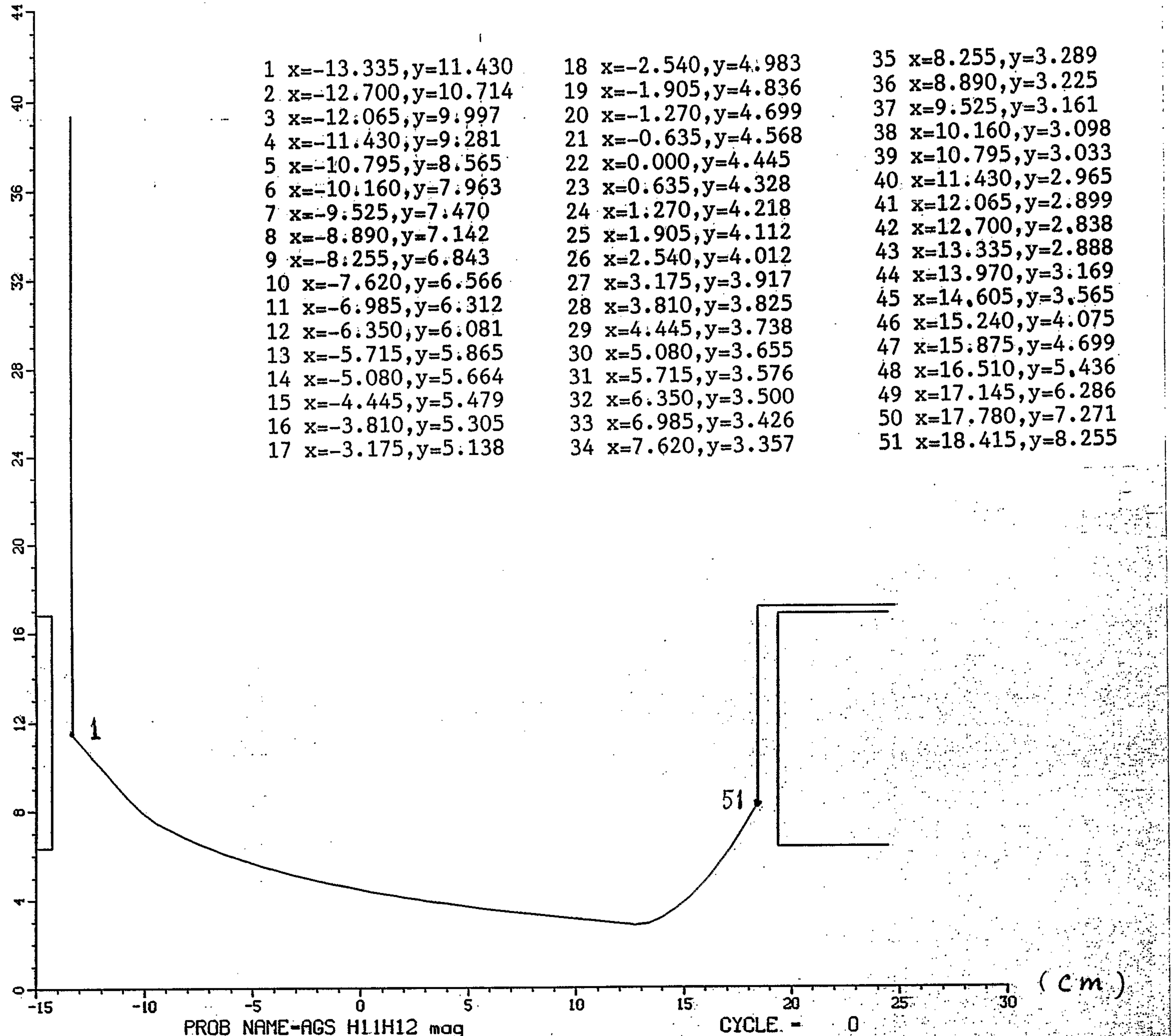

Fig.2 Pole Face

Fig. 3 and 4 Field and Gradient

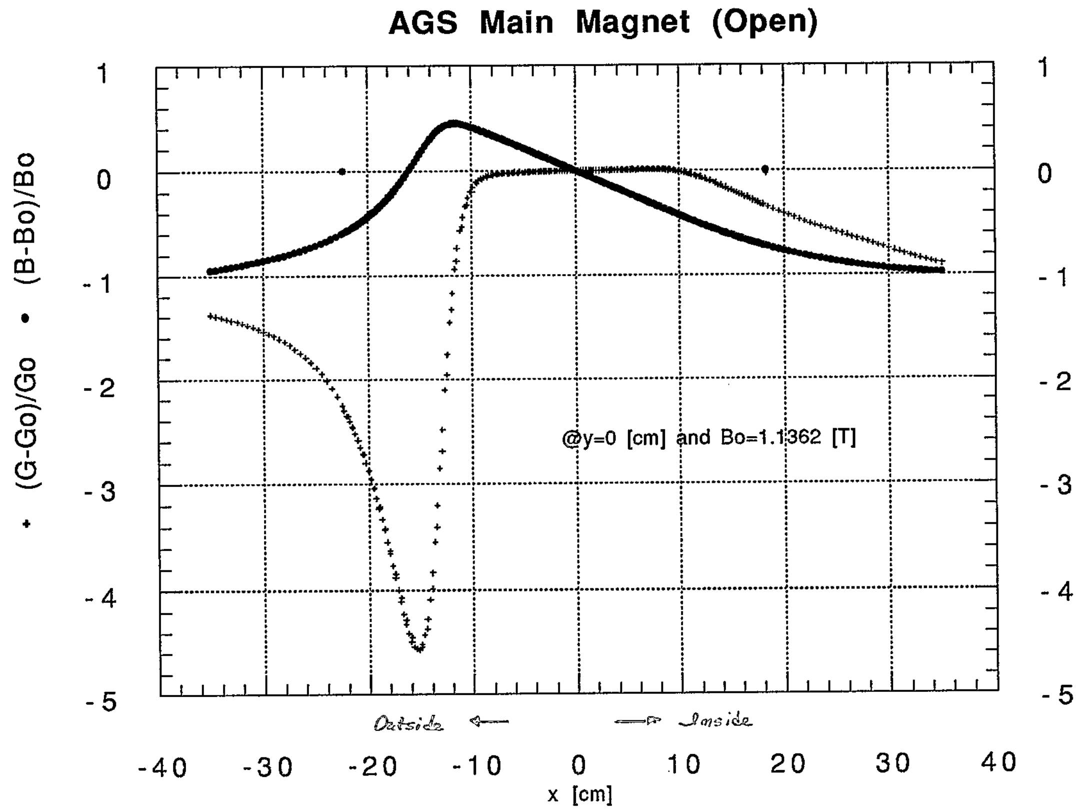

Fig.3 Open Type

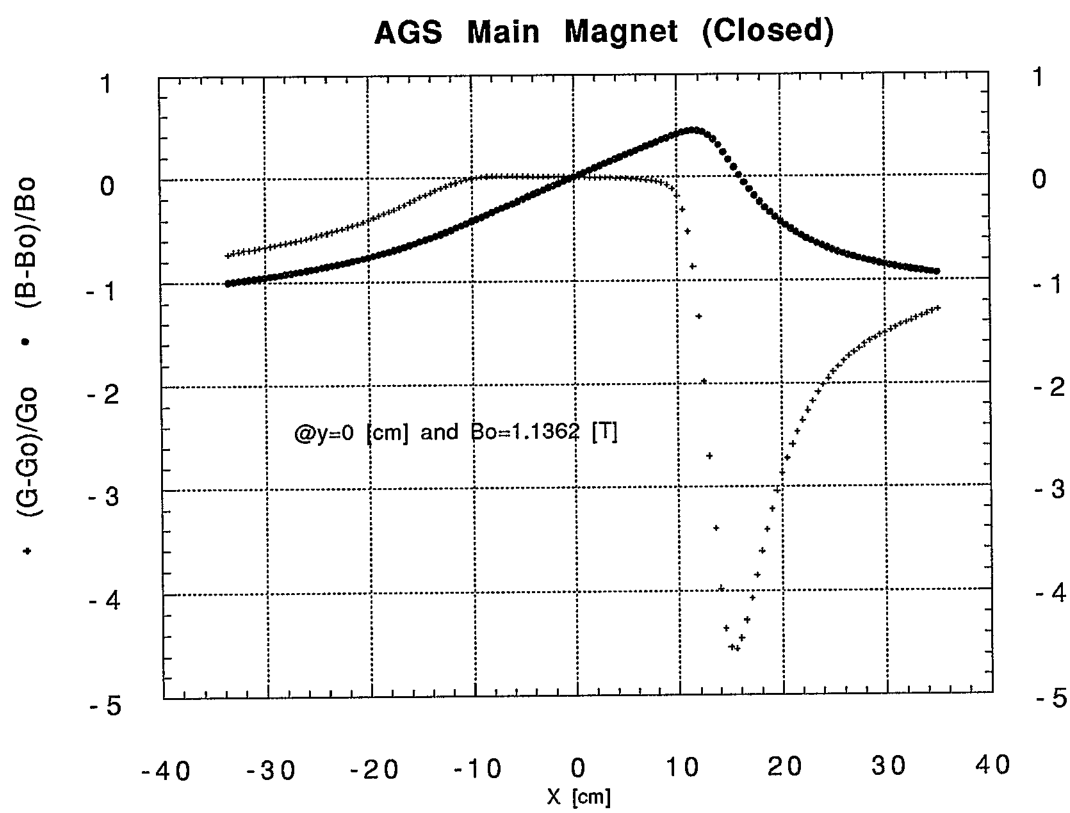

Fig. 4 Closed Type

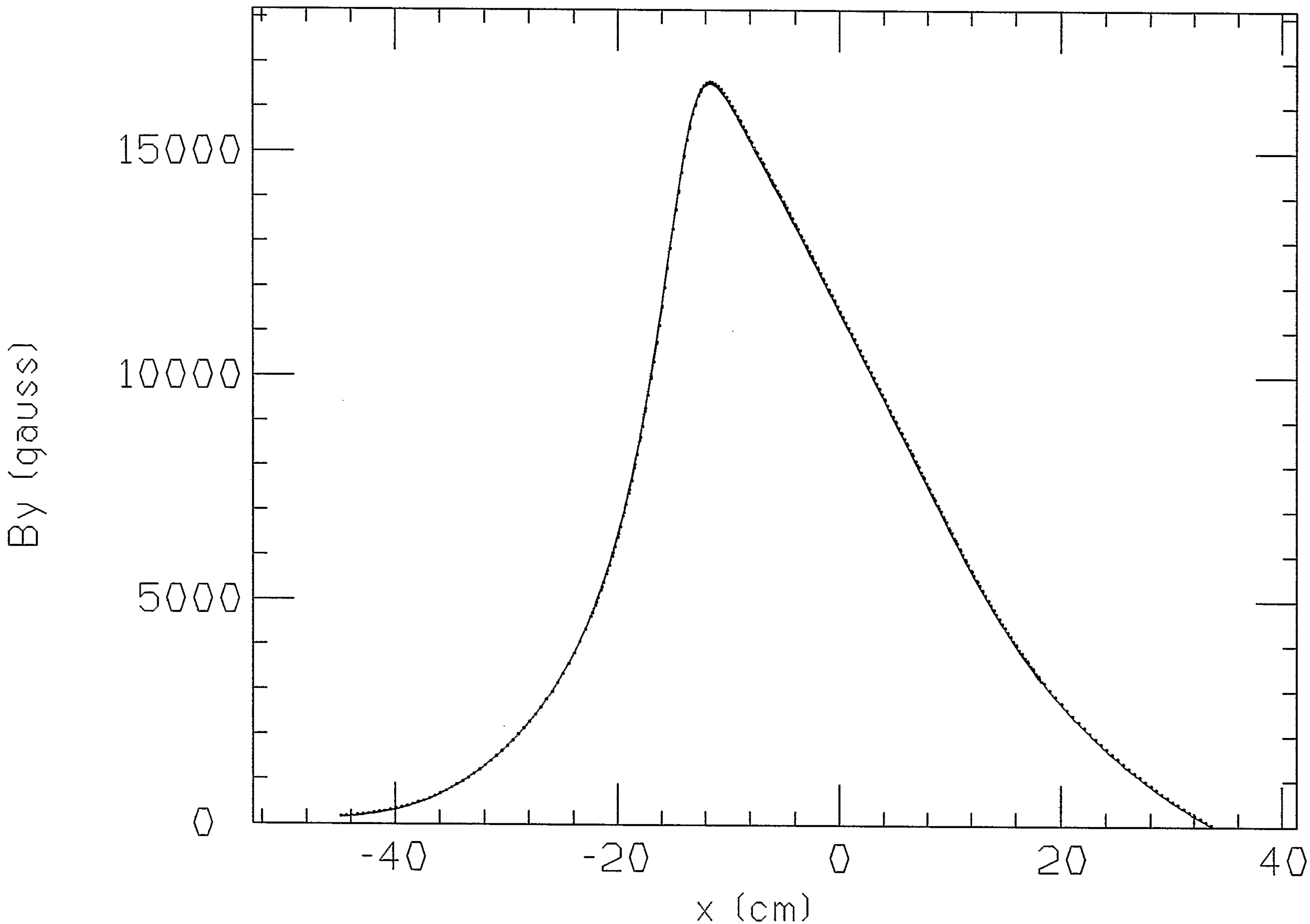

Fig.5   Compare 2d Calculation with Measurement

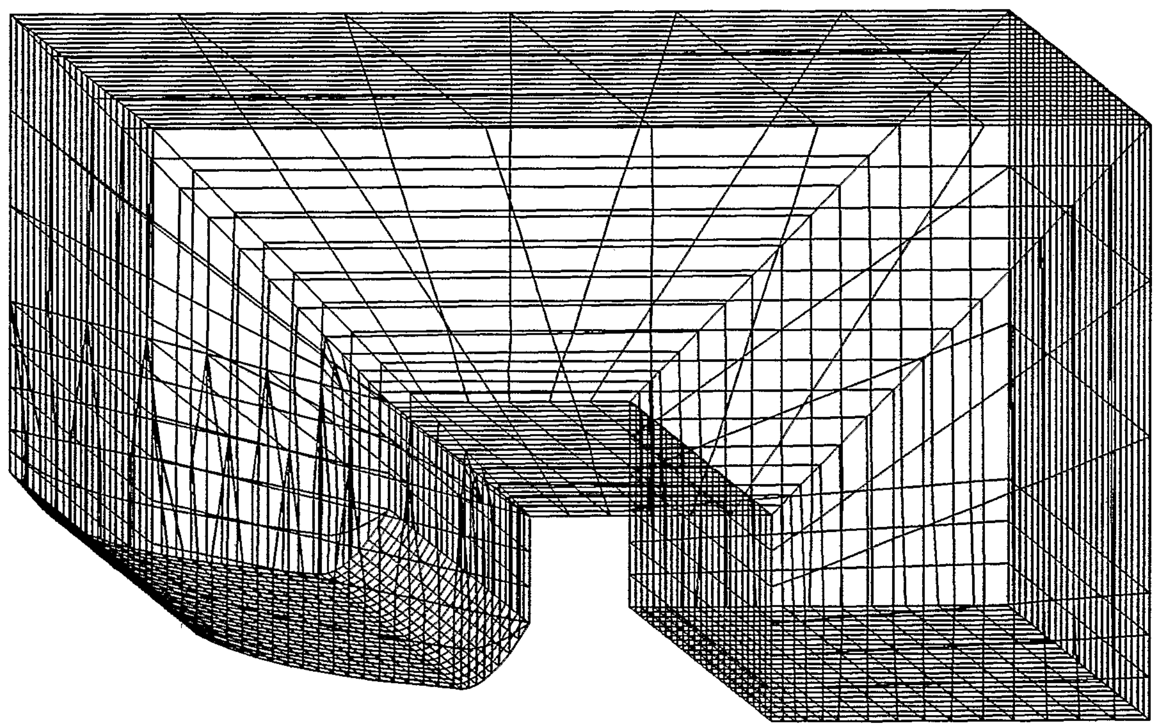

Fig.6 3d Model (Elelments are not Shown)

VF/OPERA-3d
(Post-processor)

bore.by
5/Jan/93 12:39:15 Page 7 : hist comp=by

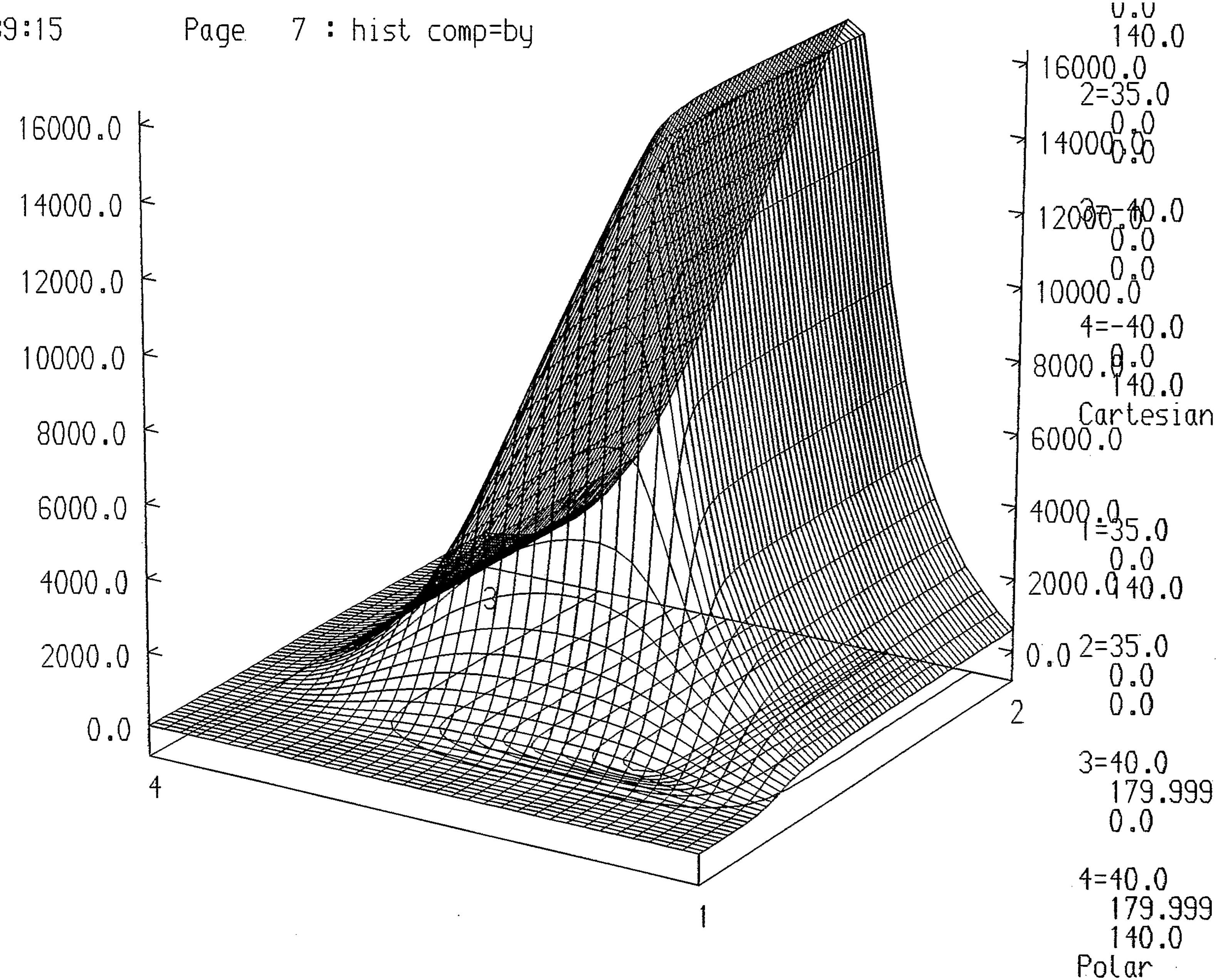

Component: BY
Maximum = 16349.5, Minimum = -9.61995
Integral = 45553172.0

Fig. 7 Landscape plot (I)

VF/OPERA-3d
(Post-processor)

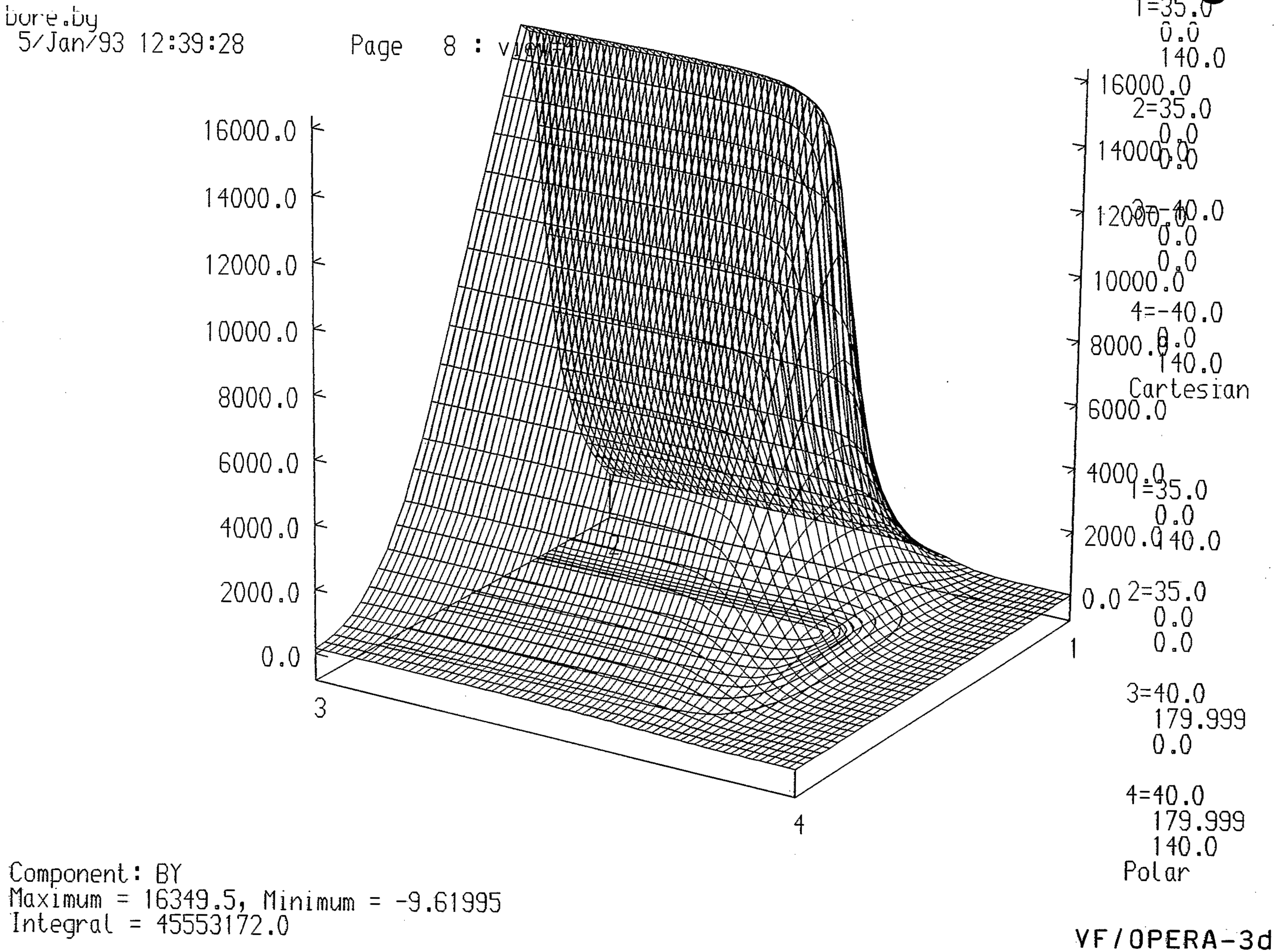

Fig. 8(a) Landscape Plot (II)

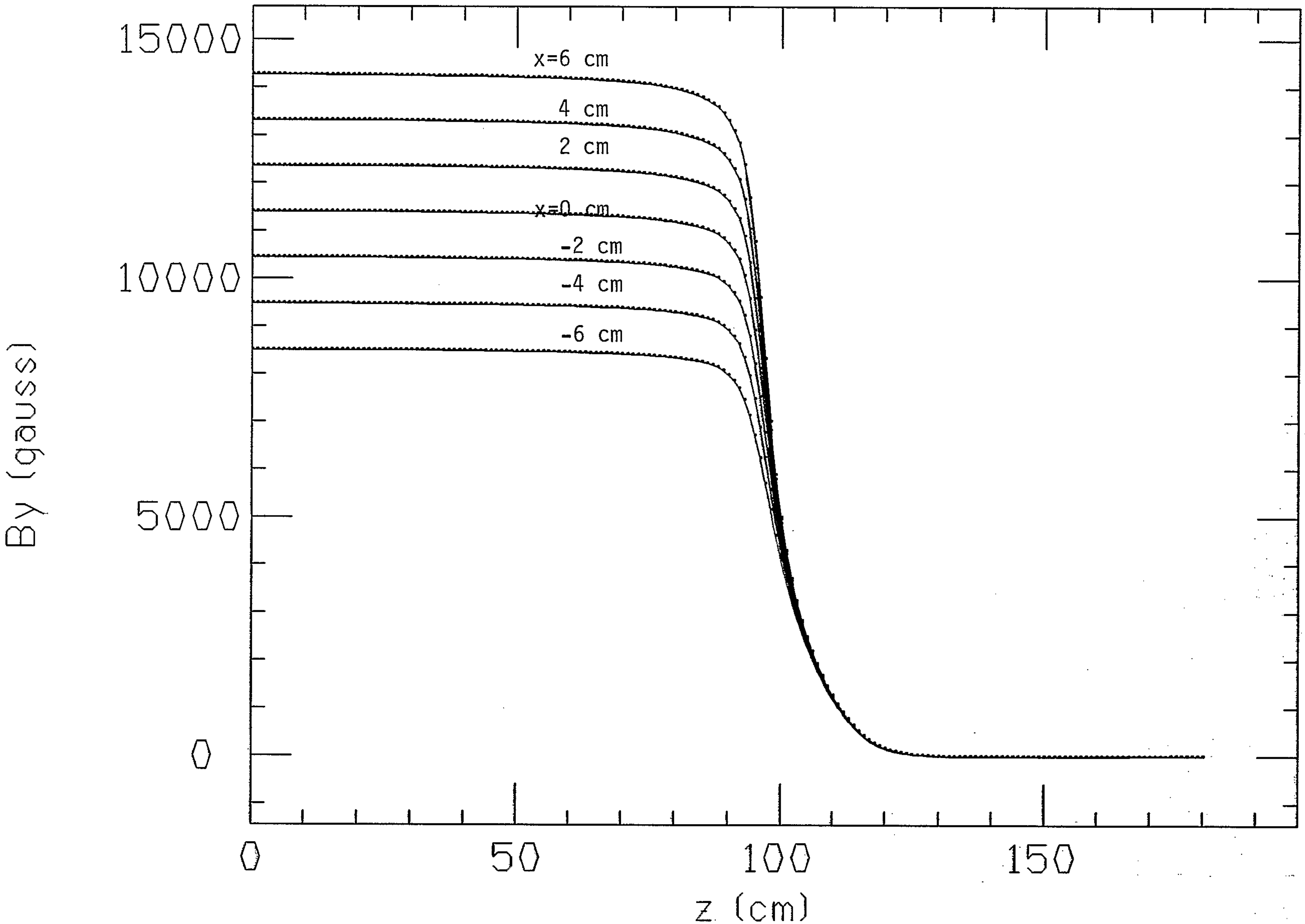

Fig.8(b) Field Profile

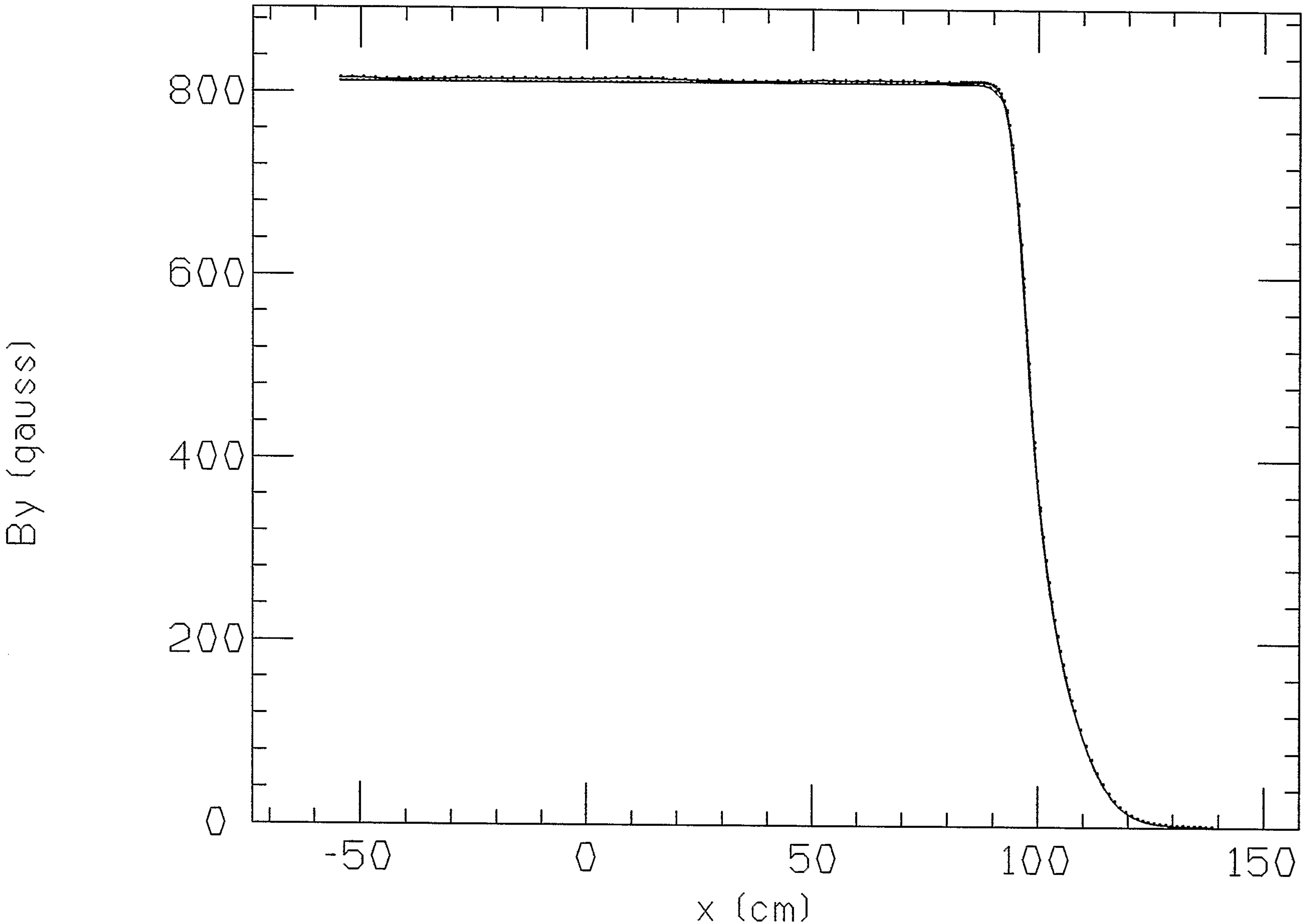

Fig.9 Comparison along the Beam Line

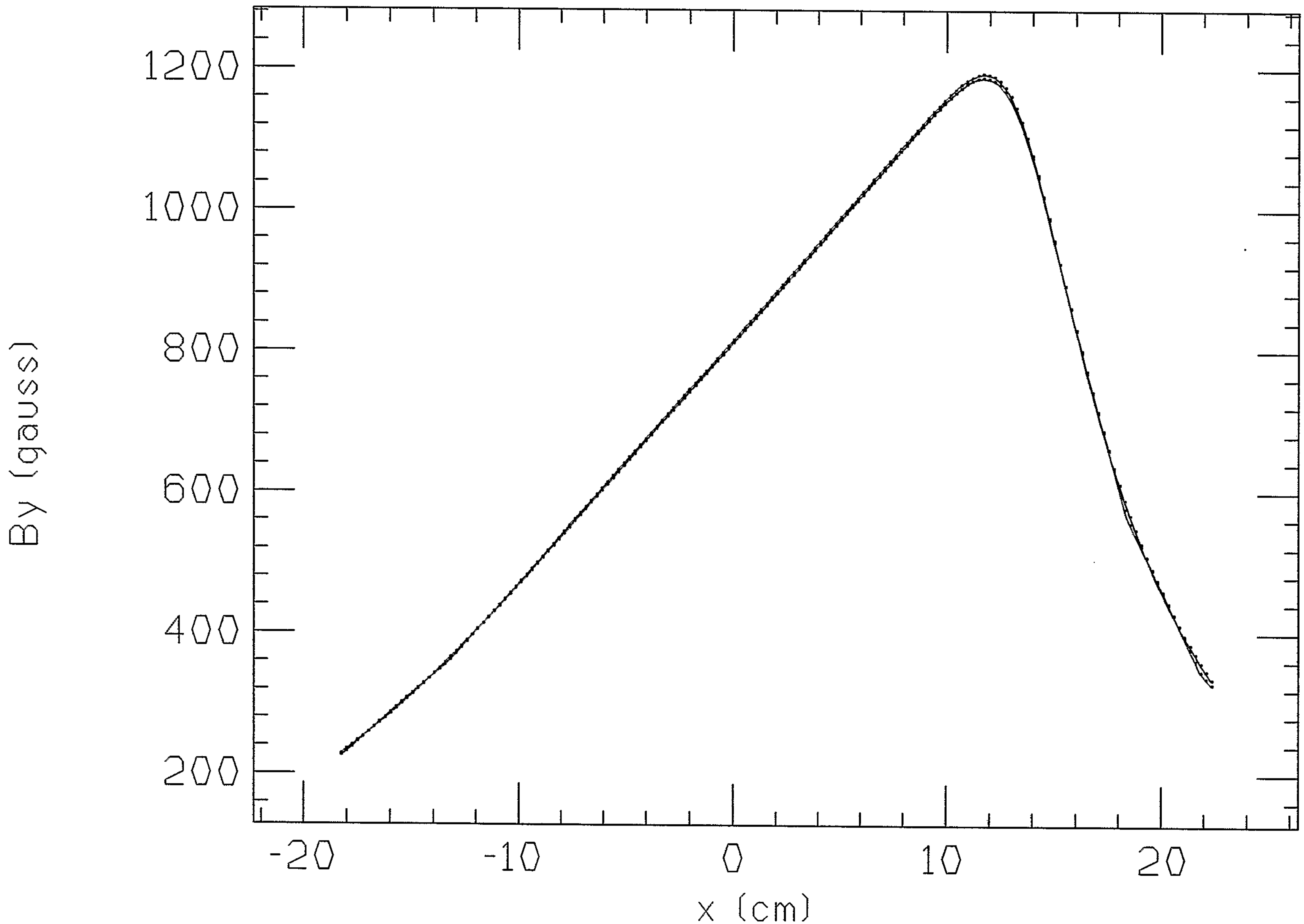

Fig. 10   Comparison near the Center (Low Field)

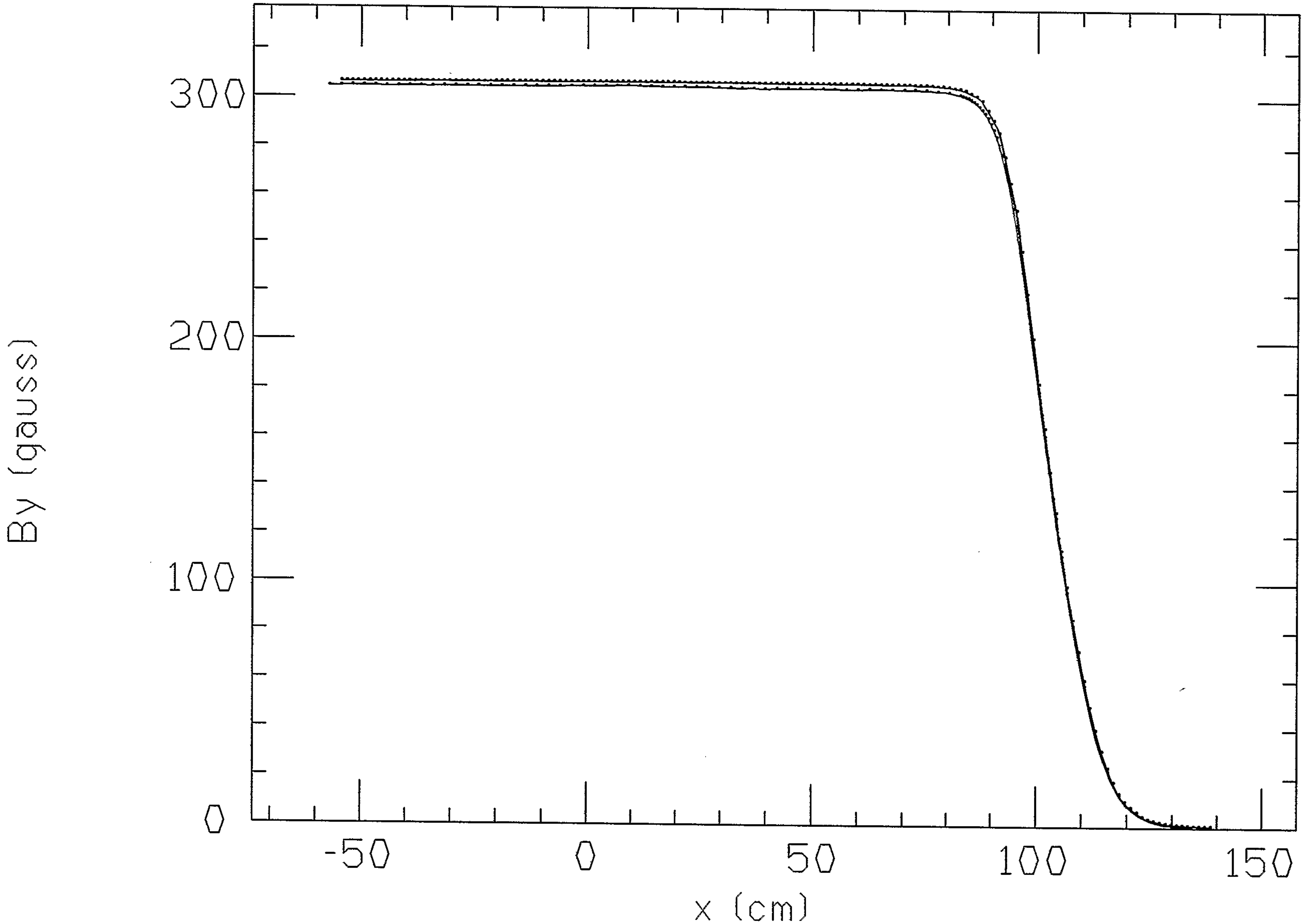

Fig. 11 Comparison in the Fringe Field Region (Low Field)

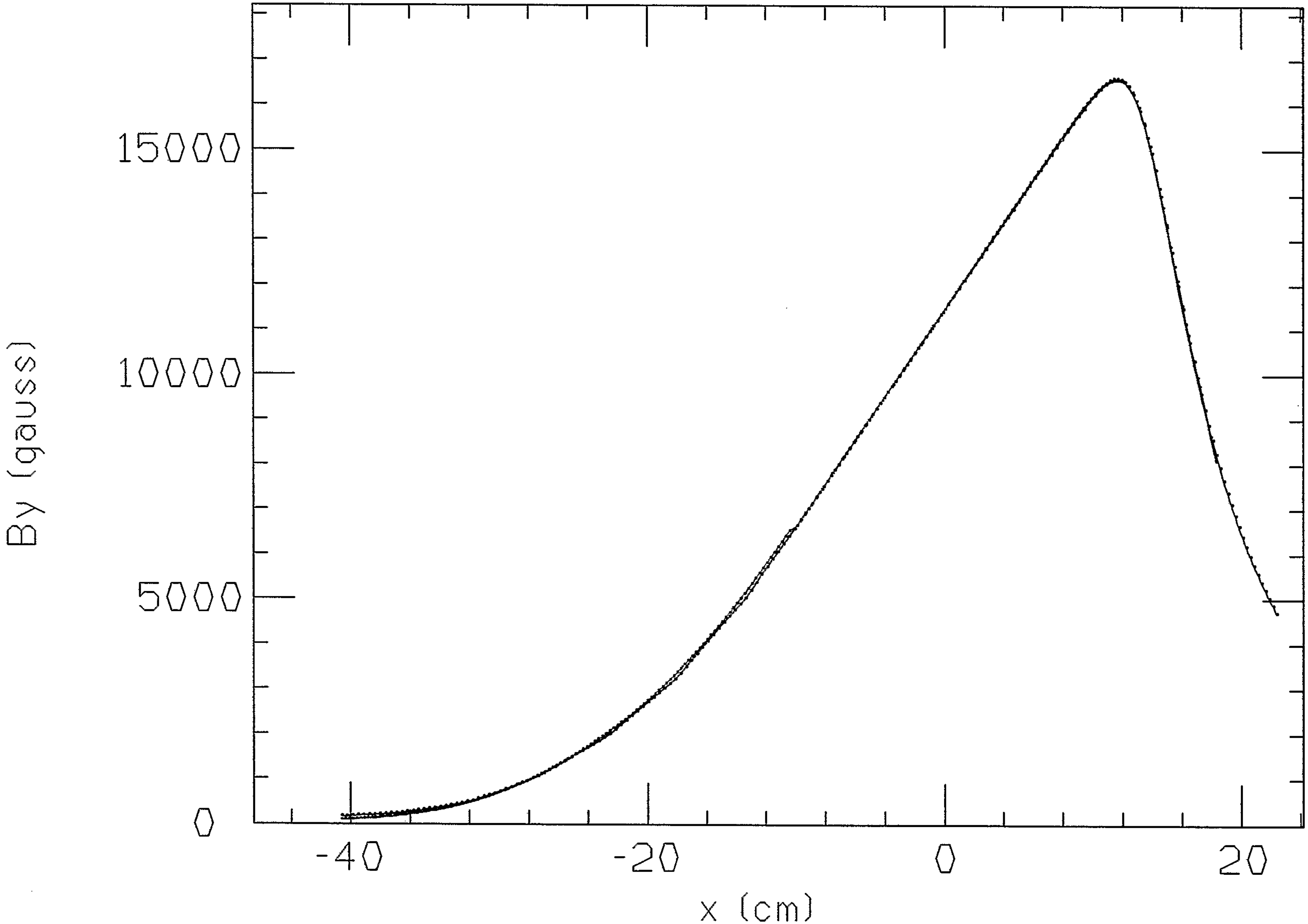

Fig. 12 Comparison near the Center (High Field)